

Application of spectroscopic methods in mineralogical and gemmological research of gem tourmalines

Peter Bačík¹, Jana Fridrichová¹, Ján Štubňa² & Peter Antal³

¹Department of Mineralogy and Petrology, Faculty of Natural Sciences, Comenius University in Bratislava, Mlynská dolina, Ilkovičova 6, 842 15 Bratislava, Slovakia; bacikp@fns.uniba.sk,

²Institute of Gemmology, Faculty of Natural Sciences, Constantine the Philosopher University in Nitra, Nábřežie mládeže 91, 949 74 Nitra, Slovakia

³Department of Inorganic Chemistry, Faculty of Natural Sciences, Comenius University in Bratislava, Mlynská dolina, Ilkovičova 6, 842 15 Bratislava, Slovakia

AGEOS Využitie spektroskopických metód v mineralogickom a gemologickom výskume drahokamových turmalínov

Abstract: Faceted tourmaline gemstones obtained from commercial sources as elbaite were studied with non-destructive spectroscopic methods. We applied Raman spectroscopy for mineral identification and UV/Vis/NIR spectroscopy for determination of chromophores. We identified the most of samples as fluor-elbaite to elbaite by Raman spectroscopy except one sample which has likely fluor-dravitic to fluor-uvitic composition. In green elbaite tourmalines divalent iron is the most significant chromophore. Yellow-green and pink elbaite tourmaline are coloured by Mn in divalent and trivalent form, respectively. The green colour of dravitic to uvitic tourmaline is the result of absorption caused by V.

Key words: tourmaline, gemmology, chromophore, Raman spectroscopy, UV/Vis/NIR spectroscopy

1. INTRODUCTION

Tourmalines are some of the most favourite gemstones in the world mostly due to their colour variability and unique colour zoning. They can have a wide spectrum of colours including black, brown, green, yellow, blue, pink, red, and violet but can be also colourless. The most requested tourmaline species for gem processing include Li-bearing fluor-elbaite, elbaite, fluor-liddicoatite and rossmanite. However, very nicely coloured crystals of Mg-rich dravite and uvite became very popular recently.

The colour of tourmaline is the result of variable chromophores present in its structure. Moreover, the position in the structure and charge interactions between cations and anions is also important to consider. Green colour of tourmaline can be result of V and Cr presence in dravite and uvite (Schmetzler & Bank, 1979). However, in fluor-elbaite it is induced by Fe²⁺-Ti⁴⁺ intervalence charge transfer (IVCT) together with Fe²⁺ (Rossman, 2013). Blue colour of “Paraíba” elbaite is produced by Mn and Cu (Abduriyim et al., 2006) but Fe²⁺-Ti⁴⁺ IVCT can also result in blue to greyish blue colour of dravite (Bačík et al., 2012). Consequently, the determination of colourization source is a very complex problem which requires the use of spectroscopic methods. However, the investigation of faceted gemstones is limited to use non-destructive and non-invasive methods and devices to identify and describe faceted gemstones. Consequently, the gemmological research differs from the traditional mineralogical approach and standard methods for mineral identification including electron microprobe and X-ray diffraction are impracticable.

The goal of the paper is the mineral identification and determination of chromophores in faceted tourmaline gemstones

obtained from commercial sources. We applied Raman spectroscopy for mineral identification and UV/Vis/NIR spectroscopy for determination of chromophores. We used widely accessible but not very specialized analytical devices to test their use in commercial practice.

2. CRYSTAL CHEMISTRY OF TOURMALINE

Tourmaline supergroup minerals are silicates crystallizing in *R3m* spacegroup with following general formula $XY_3Z_6(T_6O_{18})(BO_3)_3V_3W$, where the most common ions (or vacancy) at each site are: $X = Na^+, Ca^{2+}, K^+$, and vacancy; $Y = Fe^{2+}, Mg^{2+}, Mn^{2+}, Al^{3+}, Li^+, Fe^{3+}$, and Cr^{3+} ; $Z = Al^{3+}, Fe^{3+}, Mg^{2+}$, and Cr^{3+} ; $T = Si^{4+}, Al^{3+}$, and B^{3+} ; $B = B^{3+}$; $V = OH^-$ and O^{2-} ; and $W = OH^-, F^-$, and O^{2-} . The nomenclature of the tourmaline supergroup by Henry et al. (2011) is based on compositional variability at the *X*, *Y*, *Z*, *W*, and *V* sites which defines classification into groups, subgroups and mineral species. The primary groups are based on occupancy of the *X* site, which yields alkali, calcic, or *X*-site vacant groups. Tourmalines have a relatively complex structure.

There are 5 different cation sites with different coordination - one tetrahedral site (TO_4), two octahedral site (ZO_6, YO_6), polyhedral site XO_9 , triangular BO_3 site, and 8 different anion sites - $O1-O8$ (Donnay & Buerger, 1950).

The most prominent feature of the tourmaline structure is the ring of six TO_4 tetrahedra dominantly occupied by Si which are connected by O anions. The apical atoms O are directed to the same ($-c$) pole of crystal (Donnay & Buerger, 1950; Barton, 1969). The rings of tetrahedra are connected to two types of octahedra - ZO_6 and YO_6 which combined form brucite layer. The ZO_6 octahedron is smaller than YO_6 octahedron and is

distorted (Henry & Dutrow, 1996). The Z site is dominantly occupied by trivalent cations, usually by Al which can be substituted by Cr, V, Fe³⁺ and also Mg (Henry et al., 2011). The Y site can accommodate larger range of valences of accessing elements as monovalent Li, divalent Fe, Mg, Mn, trivalent Fe, Al, Cr, V, and also tetravalent Ti (Henry et al., 2011). The X site with coordination number of 9 is the trigonal antiprism located along threefold symmetry axis (Henry & Dutrow, 1996). X site is usually occupied by Na and Ca but is often vacant. Triangular BO₃ groups lie parallel to the plane (0001) and connect to the vertices of ZO₆ and YO₆ octahedra. Only cation entering to the B site is B (Henry et al., 2011).

There are 31 anions in the structural formula of tourmaline. Anions occupying the vertices of polyhedra are divided into 8 sites, O1–O8. Oxygen occupies O2 and O4–O8 exclusively. The O2 site connects two Y sites and B site. The O4 and O5 sites connect two tetrahedra within T₆O₁₈ rings. The O6 site links Z and Y sites to T site, O7 position connects the Z site with T site. The B site shares O8 with the Z site. One O1 (W) site and three O3 (V) sites comprise monovalent anions OH, F, Cl⁻ or a divalent anion O²⁻ (Henry et al., 2011). The W site is located on the threefold axis located at the beginning of unit cell and represents the common vertex of three YO₆ octahedra, consequently all Y-O1 bonds are crystallographically equivalent (Hawthorne, 1996, 2002). The V site is coordinated by one Y and two Z cations forming triangular pyramid arrangement similar to the O1 position but with a different quality of bonds with cations in octahedra (Hawthorne, 1996, 2002). In the most of tourmalines, this site is occupied by OH⁻ anion except fluor-buergerite and olenite with O²⁻ (Henry et al., 2011).

3. ANALYTICAL METHODS

All 8 samples except T4 are faceted gemstones and because of that they cannot be destroyed by any preparation for analytical methods. Therefore, possibilities of analysis were limited to non-destructive spectroscopic methods. Moreover, we were not able to determine the crystal orientation of samples thus all spectra have to be treated as random.

Fourier transform Raman spectra of gemstones before and after heating in range of 4000–400 cm⁻¹ were registered on NXR FT-Raman spectrometer connected to FTIR Nicolet 6700 spectrometer with InGaAs detector and semiconductor laser (976 nm). Raman spectra were processed in OMNIC Thermo Electron Corporation software.

UV/Vis/NIR spectra of gemstones in region of 300–800 nm were measured on Jasco V-530 apparatus at room temperature on the Department of Inorganic Chemistry, Comenius University in Bratislava.

Both Raman and UV/Vis/NIR spectra were processed in Seasolve PeakFit 4.1.12 software. Bands were fitted by the Gauss function with the automatic background correction. In UV/Vis/NIR spectra, absorbance value can be interpreted as inverse value corresponding to the radiant intensity. After the application of luminous efficiency function consistent with the Stockman & Sharpe cone fundamentals (Stockman & Sharpe 2000), we

got the curve of luminous intensity which represents general approximation of colour perception by human eye that is the most sensitive to light wavelength of ca 550 nm.

4. RESULTS

Sample T1 is a rectangular cut, greyish green colour, its clarity is VVS, and T2 is a cabochon of pale green colour with clarity grade SI (significant fissure viewed from the side). T3 is a brilliant of dark green colour; it is the darkest specimen from all. T4 is an angular shape green tourmaline with blue tint and VVS clarity grade, T5 is a dark green brilliant with VS clarity, T6 is a pear cut of pale green colour and VS clarity, T7 is yellow oval with VVS clarity, T8 is a pink pear with VVS clarity grade. Clarity was graded under 10× magnifications.

4.1 UV/Vis/NIR spectroscopy and colour determination

Optical absorption spectra of all samples were measured (Fig. 1, Tab. 1). Spectrum of T1 sample shows an absorption edge at 440 nm and broad absorption band at 730 nm. T2 displays significant band at 720 nm and an absorption edge at 400 nm. In contrast spectrum of T3 shows with two broad bands at 690 and 781 nm have an absorption edge shifted to blue colour region

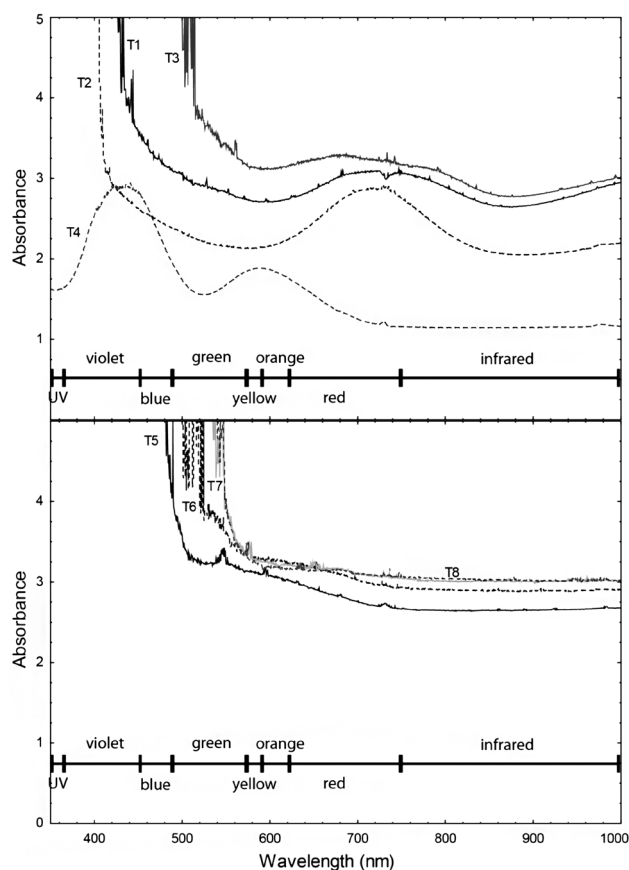


Fig. 1. UV/Vis/NIR absorption spectra of tourmaline samples.

Obr. 1. UV/Vis/NIR absorpčné spektrá turmalínov.

Tab. 1. Absorption bands in the UV/Vis/NIR absorption spectra of studied samples, their shape and absorbing cation.

Abbreviations: b – broad band; s – strong band; w – weak band.

Tab. 1. Absorpčné pásy v UV/Vis/NIR absorpčných spektrách študovaných vzoriek, ich tvar a absorbujúci kation.

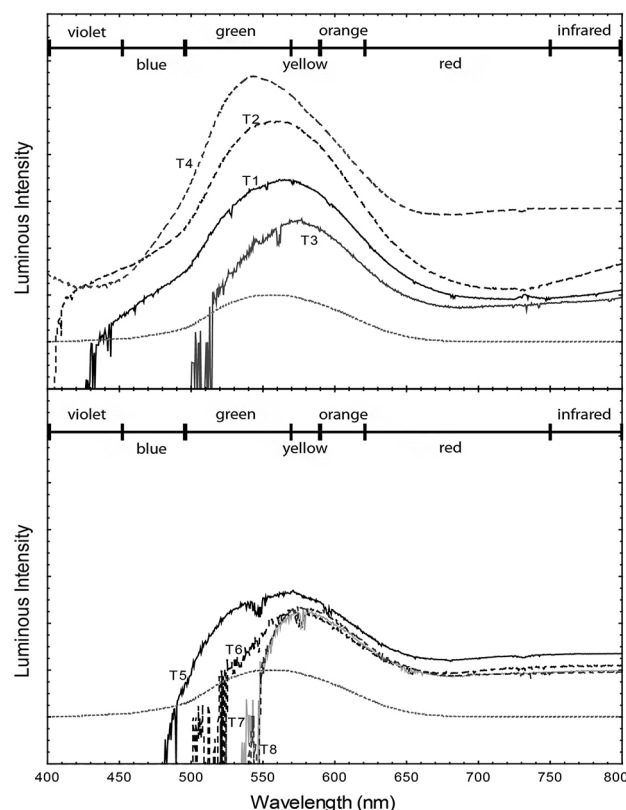
Skratky: b – široký pás; s – výrazný pás; w – slabý pás.

| | λ (nm) | band shape | cation | λ (nm) | band shape | cation | λ (nm) | band shape | cation | λ (nm) | band shape | cation, group |
|----|----------------|------------|--------------------|----------------|------------|--------------------|----------------|------------|--------------------|----------------|------------|-----------------|
| T1 | 730 | b | Fe ²⁺ | | | | | | | | | |
| T2 | 720 | s | Fe ²⁺ | | | | | | | | | |
| T3 | 690 | b | Fe ²⁺ | 781 | b | Fe ²⁺ | | | | | | |
| T4 | 434 | s | V ³⁺ | 598 | s | V ³⁺ | | | | 977 | w | OH ⁻ |
| T5 | 546 | w | Fe ²⁺ ? | 555 | w | Fe ²⁺ ? | 595 | w | Fe ²⁺ ? | | | |
| T6 | 577 | w | Fe ²⁺ ? | 652 | w | Fe ²⁺ ? | | | | | | |
| T7 | 577 | w | Mn ²⁺ ? | 651 | w | Mn ²⁺ ? | | | | | | |
| T8 | 572 | w | Mn ³⁺ ? | 633 | w | Mn ³⁺ ? | | | | | | |

at 500 nm. The absorption minimum is in the green region at 560–580 nm and the low-absorption area is relatively narrow resulting in the deep green colour without any significant tint. Sample T4 is different to all previous; it exhibits two strong bands at 434 and 598 nm. These two bands are in violet to blue and yellow region, respectively. Spectra of T5–T8 samples shows no significant bands, only several minor bands with variable position. The position of the absorption edge is likely the most important factor which decides in macroscopic colour of tourmaline. It is located between 500–550 nm in green T5 and T6, while it is shifted to around 580–600 nm in yellowish green T7 samples and pink T8 sample.

After the application of luminous efficiency function on the absorption spectra, we were able to explain variations in the studied tourmaline colour by the behaviour of the luminous intensity curve (Fig. 2). All green samples (T1–T6) display the highest luminous intensity in the green region. Different tint of green results from the variable position of the luminous-intensity maximum and also the width of each peak. The colour saturation and brightness is the function of luminous intensity. The maximum of T1 (562 nm), T2 (561 nm) and T3 (574 nm) samples is nearer to yellow region than that of T4 sample. Consequently, yellow tinge is present in T1–T3 green colour. The luminous intensity of these samples is consistent with their apparent brightness. The T2 is the brightest and the most translucent, T3 is the darkest. T4 is emerald green as the result of luminous-intensity maximum position near the centre of green region (544 nm) with higher luminous intensity in blue region compared to other samples. The T5 sample is similar to T1 in colour resulting from the position of the luminous-intensity maximum (555 nm) and the shape of the luminous-intensity curve but with slightly lower luminous intensity and apparent brightness of the stone. However, this could be also influenced by different cut. The T6 sample has very low luminous intensity in blue region and the position of maximum shifted to the border of green and yellow region (575 nm) but this could be caused by scattering of light in the cut stone because the colour of the stone does not show any visible yellow tinge. The last two samples T7 and T8 are different

in colour compared to others. Yellow colour of T7 complies with the position of luminous intensity maximum (580 nm) in yellow region. The luminous intensity curve of pink T8 sample with maximum at 582 nm is very similar to T7 which could suggest that its shape could be altered by the absorption and light scattering effects mostly in the violet region.

**Fig. 2.** Luminous-intensity curves of light transmitted through tourmaline samples. Dotted line is for the luminous efficiency function (Stockman & Sharpe, 2000) applied on calculation of luminous-intensity curves.

Obr. 2. Krivky intenzity svetla prechádzajúceho vzorkami turmalínov. Bodkovaná čiara reprezentuje funkciu svietivosti (Stockman & Sharpe, 2000) použitú na výpočet kriviek intenzity svetla.

4.2 Raman spectroscopy

It was possible to get Raman spectra only from seven samples (Fig. 3). The spectra of T3 sample gave no Raman-active bands which might be attributed to strong dispersion of laser light on faceted gemstone. All other spectra were inspected on the presence of Si-O, B-O and O-H vibrations (Tabs. 2, 3) and are similar to published tourmaline spectra (RRUFF, 2014). The bands in spectra were interpreted according to Hoang et al. (2011) and Reddy et al. (2007). However, the presence and intensity of Raman bands is influenced by unknown crystallographic orientation of cut gemstones and spectra are altered by luminescence effects.

It is possible to indirectly determine the occupancy of octahedral sites from the location of O-H bands. Bands between 3470 and 3590 cm^{-1} result from $^{\text{V}}\text{OH}$ vibrations, while those with wavenumber higher than 3600 cm^{-1} are induced by $^{\text{W}}\text{OH}$ vibrations. The bands at 3470–3484 cm^{-1} in samples T1, T2, and T3 can be interpreted as composite vibrations $^{\text{V}}\text{OH}$ surrounded by two $^{\text{Z}}\text{Al}$ and $^{\text{Y}}\text{Al}$ or $^{\text{Y}}\text{Li}$. The bands at 3515–3521 cm^{-1} in samples T5 and T8 are likely produced by $^{\text{V}}\text{OH}$ surrounded

by two $^{\text{Z}}\text{Al}$ and $^{\text{Y}}\text{Li}$. All samples contain band at 3553–3582 cm^{-1} , which could result from $^{\text{V}}\text{OH}$ vibrations in the $^{\text{Z}}\text{Al}^{\text{Z}}\text{Al}^{\text{Y}}\text{Mg}$ environment typical for Mg-dominant tourmalines such as dravite or uvite.

The $^{\text{W}}\text{OH}$ vibrations are in two regions; in the T1 and T2 samples the vibrations between can be attributed to OH surrounded by $^{\text{Y}}\text{Al}^{\text{Y}}\text{Al}^{\text{Y}}(\text{Al}, \text{Li})$. In contrast, in the T4–T7 samples $^{\text{W}}\text{OH}$ site hydroxyl group is in the $^{\text{Y}}\text{Mg}^{\text{Y}}\text{Mg}^{\text{Y}}(\text{Al}, \text{Mg})$ environment. The minute intensity of $^{\text{W}}\text{OH}$ vibrations in the T1 and T2 samples can be attributed to dominance of fluorine in the $^{\text{W}}$ site which is typical for fluor-elbaite. Therefore, these samples can be interpreted as these mineral species. The location of $^{\text{W}}\text{OH}$ vibrations in the T5–T7 samples suggests that they could contain increased dravitic component but also likely belong to fluor-elbaite. The T8 sample similarly to T1 and T2 displays very weak $^{\text{W}}\text{OH}$ band at 3648 cm^{-1} (the shoulder on 3579 cm^{-1} band), therefore, it also most likely can be fluor-dravite. The T4 sample is completely different with no OH vibrations in Li-bearing environment; those in the Mg-bearing environment are dominant. Consequently, this sample is dravite or uvite very likely.

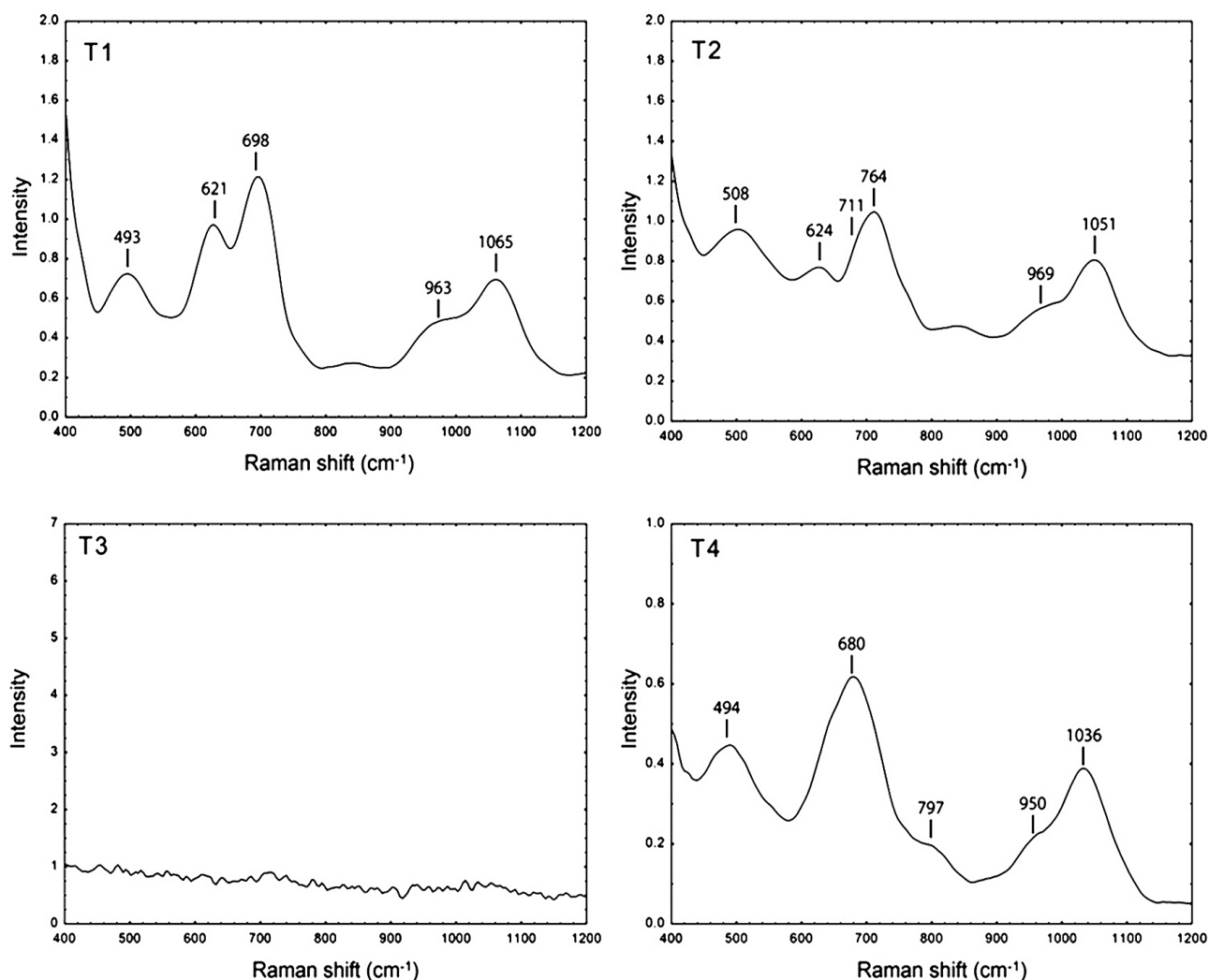


Fig. 3. Raman spectra of internal vibrations bands in tourmaline samples.

Obr. 3. Ramanove spektrá s vnútorými vibráciami turmalínov.

Tab. 2. Wavenumber (in cm^{-1}) of internal vibrations bands in the Raman spectra of studied samples.Abbreviations: O_{non} – non-bridging oxygen in tetrahedral ring, O_{br} – bridging oxygen in tetrahedral ringTab. 2. Vlnočet (v cm^{-1}) pásov vnútorných vibrácií v Ramanových spektrách študovaných vzoriek.Skratky: O_{non} – atómy O neprepájajúce tetraédre TO_4 v rámci prstenca, O_{br} – atómy O prepájajúce tetraédre TO_4 v rámci prstenca

| | T1 | T2 | T4 | T5 | T6 | T7 | T8 |
|--|------|------|------|------|------|------|------|
| symmetric stretching of (Si-O) ring | 493 | | 494 | 484 | 475 | 479 | |
| symmetric stretching of (Si-O) ring | | 508 | | | | | 513 |
| asymmetric stretching of (Si-O) ring | 621 | 624 | | 614 | 651 | 632 | 617 |
| asymmetric stretching of (Si-O) ring | 698 | | 680 | 692 | 683 | | |
| asymmetric stretching of (Si-O) ring | | 711 | | | 714 | 706 | 714 |
| (BO_3) deformation | | 764 | 797 | 799 | 775 | 792 | |
| Si-O stretching | 963 | 969 | 950 | 964 | 966 | 956 | 982 |
| Si- O_{non} stretching | | | | | 1024 | | |
| Si- O_{br} stretching | 1065 | 1051 | 1036 | 1067 | 1049 | 1051 | 1055 |
| Si- O_{br} stretching | | | | | 1089 | | |

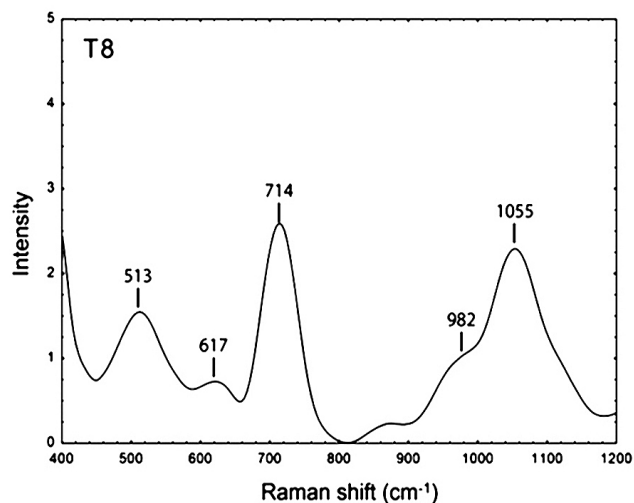
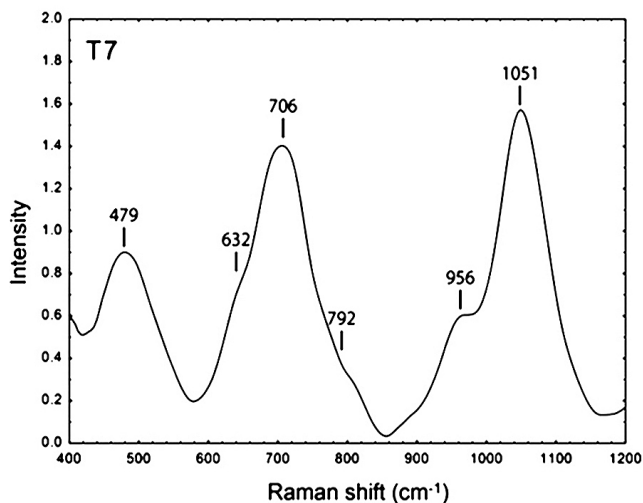
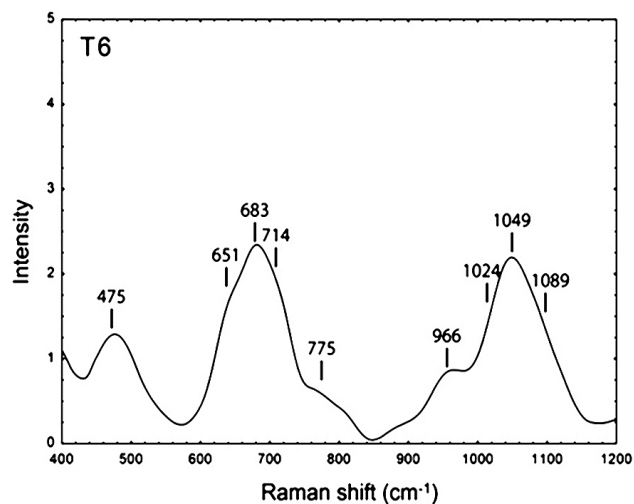
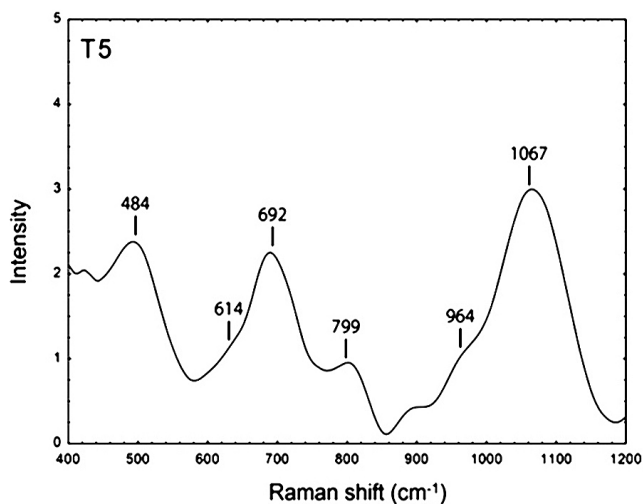


Fig. 3. continued

Obr. 3. pokračovanie

Tab. 3. Wavenumber (in cm^{-1}) and intensity of O-H bands in the Raman spectra of studied samples.Abbreviation: l.e. – local environment; ν – wavenumber (in cm^{-1}); I – intensityTab. 3. Vlnočť (ν cm^{-1}) pásov vibrácií O-H väzieb v Ramanových spektrách študovaných vzoriek.Skratky: l.e. – lokálne usporiadanie pozície, ν – vlnočť (in cm^{-1}); I – intenzita

| site | V | | V | | V | | W | | W | |
|------|---|------|---|------|---|------|---|------|---|------|
| | ${}^z\text{Al}{}^z\text{Al}{}^y(\text{Al},\text{Li})$ | | ${}^z\text{Al}{}^z\text{Al}{}^y\text{Li}$ | | ${}^z\text{Al}{}^z\text{Al}{}^y\text{Mg}$ | | ${}^y\text{Al}{}^y\text{Al}{}^y(\text{Al},\text{Li})$ | | ${}^y\text{Mg}{}^y\text{Mg}{}^y(\text{Al},\text{Mg})$ | |
| | ν | I | ν | I | ν | I | ν | I | ν | I |
| T1 | 3484 | 0.63 | - | - | 3570 | 1.29 | 3677 | 0.04 | - | - |
| T2 | 3470 | 0.13 | - | - | 3579 | 0.36 | 3649 | 0.06 | - | - |
| T3 | - | - | - | - | - | - | - | - | - | - |
| T4 | - | - | - | - | 3553 | 0.49 | - | - | 3730 | 0.05 |
| T5 | - | - | 3515 | 0.95 | 3557 | 1.25 | - | - | 3717 | 0.21 |
| T6 | - | - | - | - | 3567 | 2.94 | - | - | 3724 | 0.22 |
| T7 | - | - | 3521 | 0.23 | 3567 | 1.18 | - | - | 3715 | 0.06 |
| T8 | 3470 | 1.23 | - | - | 3579 | 1.41 | 3648 | 0.12 | - | - |

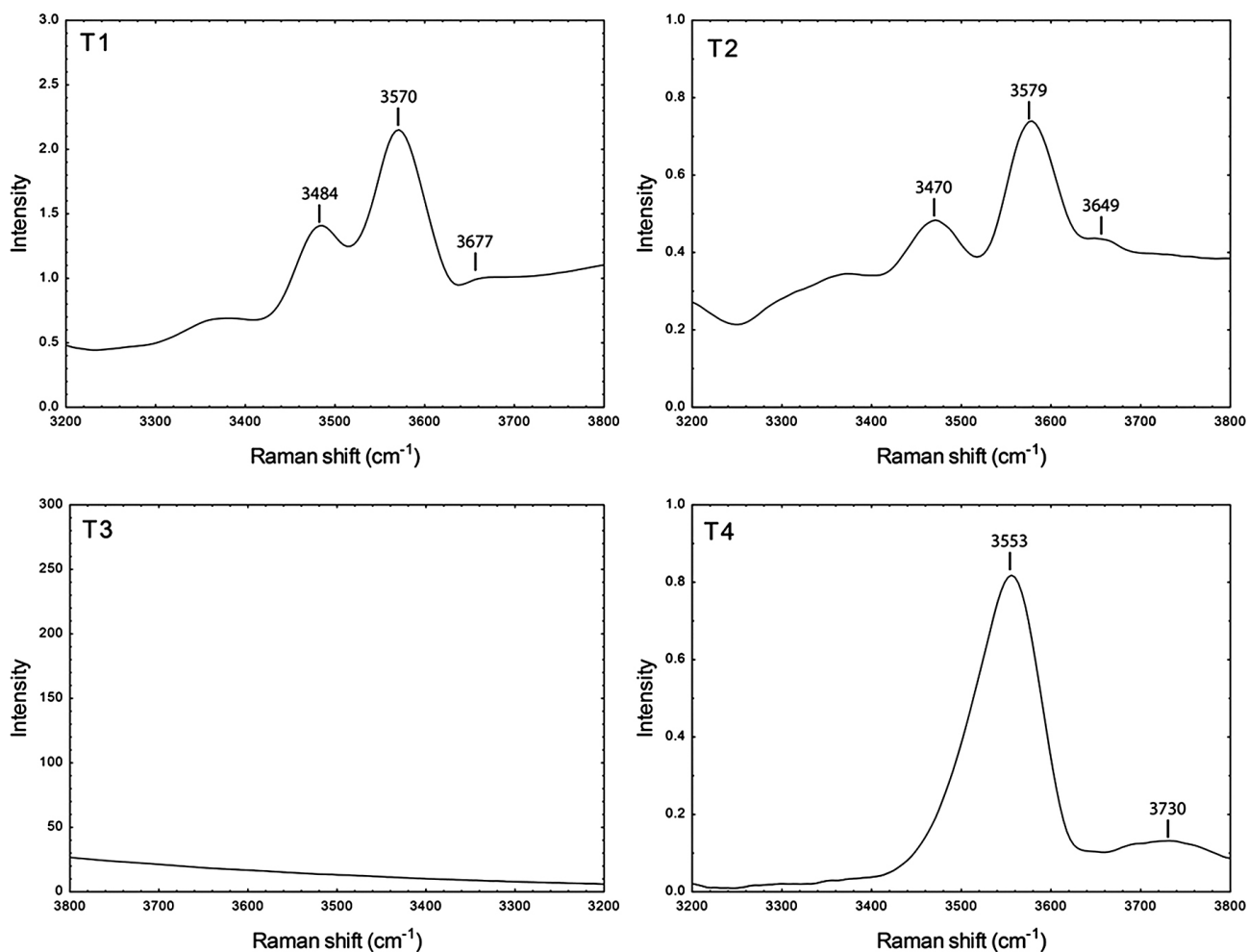


Fig. 4. Raman spectra of O-H vibrations bands in tourmaline samples.

Obr. 4. Ramanove spektrá s vibráciami O-H väzieb turmalínov.

5. DISCUSSION AND CONCLUSION

5.1. Causes of tourmaline colour

The understanding of mineral colour is a relatively complicated issue. Firstly, it is necessary to define colour itself. For our purposes we can specify whether the colour belongs to the spectral sequence or is non-spectral such as purple, magenta, or pink. This attribute is variously designated in different descriptive systems as *hue*, *dominant wavelength*, *chromatic colour*, or simply but quite imprecisely as *colour*. Spectral colours can be defined by their wavelength. Non-spectral colours are, in contrast, result of colour mixing. The relationship between observed colour and the spectral wavelength is not straightforward. For example, the same perception of pink is given by: (a) an unsaturated reddish-orange mixed with some white light; (b) a mixture of beams of red with cyan; (c) a mixture of red, green, and violet beams; and so on (Nassau, 1998). Therefore, it is impossible to determine the exact distribution of dominant wavelengths contributing to specific colour and optical absorption spectra is necessary for their determination.

The factors causing mineral colour can be divided to five groups: (1) metal ions in the structure; (2) intervalence charge transfer involving metal ions in mixed oxidation states, most commonly $\text{Fe}^{2+} - \text{Fe}^{3+}$ and $\text{Fe}^{2+} - \text{Ti}^{4+}$ interaction; (3) natural and artificial ionizing radiation; (4) physical effects such as optical diffraction; (5) band gaps in semiconducting minerals (Rossman, 2013). First two causes are the most commonly responsible for the colour of tourmalines. However, wide variability in tourmaline colour is possible only if the most intensively absorbing chromophores including Fe and Ti are in minor to trace amounts. High absorption by high Fe and Ti contents causes dark (macroscopically black) colour of Fe-rich tourmalines (e.g., Pieczka, 2007; da Fonseca-Zang et al., 2008).

Consequently, most of the tourmaline with not negligible Fe content including schorl and dravite is macroscopically black. However, if the content of the above-mentioned elements is low, it could result in the different tourmaline colour. Therefore, we can presume that studied samples are low in Fe and Ti.

The green colour of T1–T3 sample is caused by broad absorption bands in the red region and an increased absorption

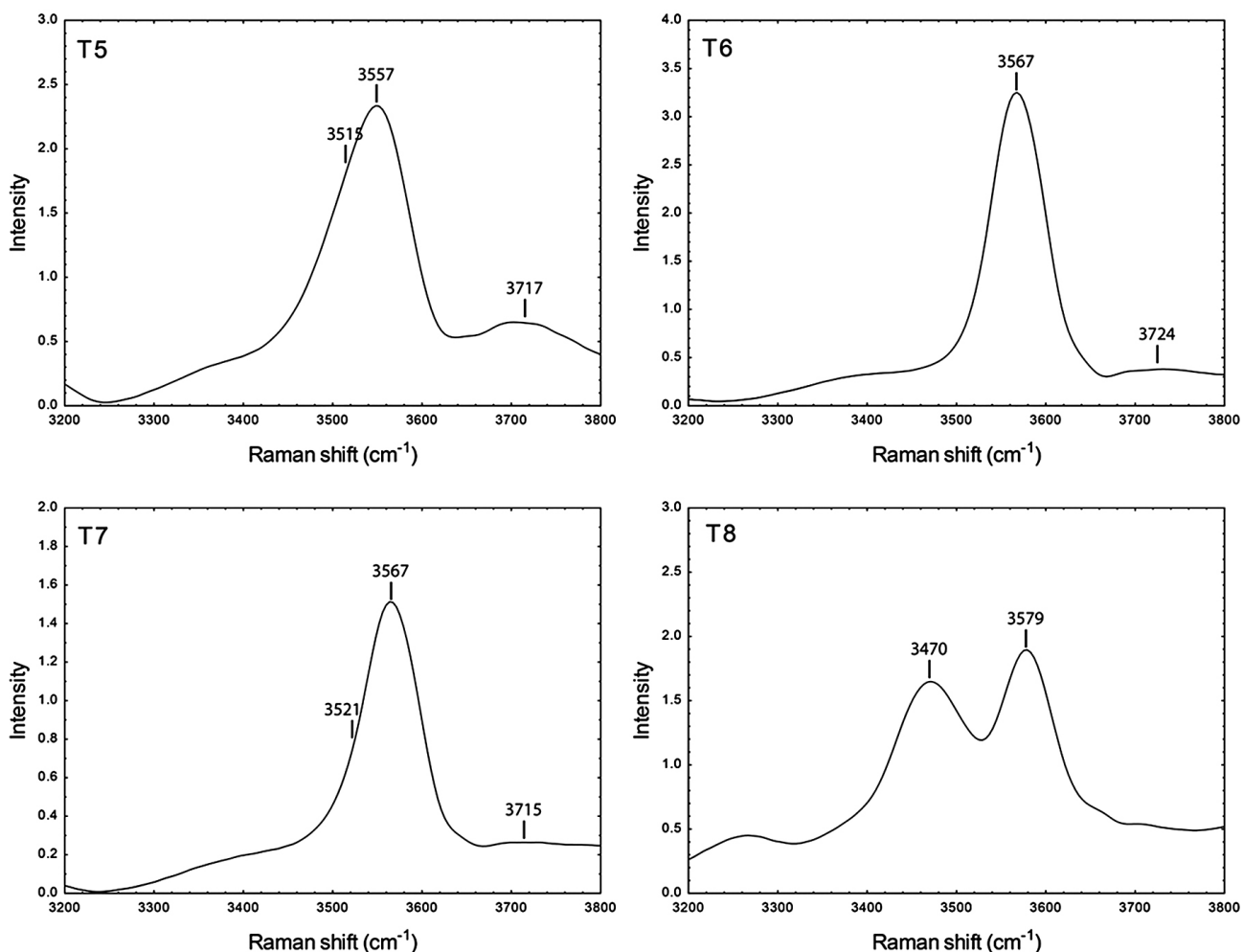


Fig. 4. continued

Obr. 3. pokračovanie

towards the absorption edge in the blue to violet region. The broad absorption bands can be attributed to Fe^{2+} (Laurs et al., 2008; Merkel & Breeding, 2009). Consequently, these samples have an elbaite composition likely, since the green colour in elbaite is often caused by Fe^{2+} . Presence of Cu^{2+} as another possible green-colour inducing chromophore can be excluded, since Cu^{2+} exhibits two significant peaks at 700 and 900 nm (Merkel & Breeding, 2009) which we did not observe. Significant increase in absorption at the T1–T3 spectra can be attributed to an overtone of OH vibrations (Rossman et al., 1991; Laurs et al., 2007) but have no influence on the colour of samples.

The T4 sample displays two strong absorption bands in the violet to blue and yellow region typical for V^{3+} and Cr^{3+} (Merkel & Breeding, 2009). Since the colour in uvite and green dravite is caused by V^{3+} and Cr^{3+} (Schmetzer & Bank, 1979) and both of them never occur in elbaite (Rossman et al., 1991), we can assume that the T4 sample is uvitic or dravitic very likely. It is also supported by the Raman spectra in which no O–H vibrations with Li neighbouring in the Y site occur and it is typical for Mg- and Fe-bearing tourmalines (Hoang et al., 2011). It is almost ruled out that this sample could be Fe-dominant, since the high Fe content results in the black colour (da Fonseca-Zang et al., 2008). Moreover, we can presume that V is dominant chromophore over Cr and the tourmaline has uvitic more likely than dravitic composition. This presumption is based on the recent data on green “dravites” or “chromedravites” (as usually distributed commercially) which are actually V-bearing uvite (Rossman, 2013; Bačík, unpublished data).

The green colour of T5 and T6 samples can also be the result of Fe presence in the structure, although it is not manifested by any significant absorption band. Moreover, their spectra can be altered by orientation, reflection and dispersion effects in cut stones resulting in worse quality of spectra. However, weak absorption bands in these samples can result from absorption on Fe^{2+} .

The T7 and T8 spectra look relatively similar although the T7 sample has a yellow colour and T8 is pink. Manganese in various oxidation states is a typical chromophore responsible for both yellow and pink colour. Yellow colour results from absorption in violet region caused by Mn^{3+} and blue to green absorption because of the Ti^{4+} and Mn^{2+} interaction (Rossman & Mattson, 1986; Ertl et al., 2012). In contrast, pink elbaite tourmaline contains significantly lower proportion of Mn^{2+} , therefore, there is significantly lower absorption in violet region and violet transmission connected with yellow-to-red can produce pink colour (Merkel & Breeding, 2009). Otherwise, the shape of absorption curve between green and red region is relatively similar. This could be the case of T7 and T8 samples with Mn as a dominant chromophore likely. However, in both samples we got very high base absorption in red-to-yellow region and absorption edge located in the green region. This can be caused by the light-scattering effects in measured gemstones. Consequently, we were not able record violet transmission in the T8 sample which is likely responsible for pink colour of this tourmaline.

5.2. Advantages and disadvantages of spectroscopic methods in the research of gems

The gemmological investigation is similar to the classical mineralogical research in some features. It addresses the same kind of samples and uses similar analytical methods. However, the need to preserve faceted gemstones limits the use methods and devices for identification and description of samples which must be non-destructive and non-invasive. Spectroscopic methods are very appropriate since they do not require any specialized sample preparation, do not alter the sample in any way and can also be used as portable.

However, there are also some limits in their use. Most of them are based on the type and properties of samples. Gemstones are usually faceted and individual facets are inclined in variable angles. Consequently, they produce reflections inside the gemstones which refract and disperse light influencing the total absorption. Laser beam with specific wavelength used in Raman spectroscopy can induce photoluminescence that produce artefacts in the Raman spectra (Nasdala et al., 2004). Moreover, the interpretation of Raman and further UV/Vis/NIR spectra is more appropriate with the direct crystallographic orientation which is also limited in faceted gemstones. It is recommended to measure in directions parallel or perpendicular to the Z axis (Laurs et al., 2008; Merkel & Breeding, 2009). These directions correspond to minimal (parallel to Z axis) and maximal (perpendicular to Z axis) absorption. Tourmaline has a significant pleochroism (darkest colour is visible in the direction of ordinary ray – perpendicular to Z axis, or parallel – but only in the direction of the ordinary ray). The darkest colour results from the highest absorption. This can be explained by the geometrical arrangement of chromophore-bearing octahedral sites. In the Z-axis direction, octahedral Y sites containing usually most of chromophores occupy larger area than in the view perpendicular to the Z. Consequently, the probability of light absorption in the direction parallel to Z on Y-site cations is higher than in the perpendicular direction which explains the differences in absorption in different directions. These are reasons limiting spectroscopic methods in their use on faceted gemstones.

Finally, the exact determination of gemstone chemical composition is very complicated. Electron microprobe cannot be usually used since the gemstone is not suitable for standard preparation. Moreover, samples analyzed by electron microprobe have to be covered by conductive material which could alter the cleanness of gemstone surface. For more detailed analysis it is possible to use other non-destructive techniques, e.g., XRF but they have lower accuracy of analysis.

Acknowledgement: Authors are indebted to Andreas Ertl and Igor Broska for their detail reviews and Martin Ondrejka and Rastislav Vojtko for editorial handling.

6. REFERENCES

- Abduriyim A., Kitawaki H., Furuya M. & Schwarz D., 2006: Paraiba-type copper-bearing tourmaline from Brazil, Nigeria, and Mozambique: Chemical fingerprinting by LA-ICP-MS. *Gems & Gemology*, 42, 1, 4–21.

- Bačík P., Uher P., Cempírek J. & Vaculovič T., 2012: Magnesian tourmalines from plagioclase-muscovite-scapolite metaevaporite layers in dolomite marble near Prosetín (Olešnice Unit, Moravicum, Czech Republic). *Journal of Geosciences*, 57, 143–153.
- Barton P. Jr., 1969: Refinement of the crystal structure of buergerite and the absolute orientation of tourmalines. *Acta Crystallographica*, B52, pp. 1524–1533.
- da Fonseca-Zang W.A., Zang J.W. & Hofmeister W., 2008: The Ti-influence on the tourmaline colour. *Journal of the Brazilian Chemical Society*, 19, 1186–1192.
- Donnay G. & Buerger M.J., 1950: The determination of the crystal structure of tourmaline. *Acta Crystallographica*, 3, 5–12.
- Ertl A., Kolitsch U., Dyar M.D., Hughes J.M., Rossman G.R., Pieczka A., Henry D.J., Pezzotta F., Prowatke S., Lengauer C.L., Körner W., Brandstätter F., Francis C.A., Prem M. & Tillmanns E., 2012: Limitations of Fe²⁺ and Mn²⁺ site occupancy in tourmaline: Evidence from Fe²⁺- and Mn²⁺-rich tourmaline. *American Mineralogist*, 97, 1402–1416.
- Hawthorne F. C., 1996: Structural mechanisms for light elements in tourmaline. *Canadian Mineralogist*, 34, 123–132.
- Hawthorne F. C., 2002: Bond-valence constraints on the chemical composition of tourmaline. *Canadian Mineralogist*, 40, 789–797.
- Henry D.J. & Dutrow B.L., 1996: Metamorphic tourmaline and its petrologic applications. In: Grew E.S. & Anowitz L.M. (Eds.): Boron. Mineralogy, petrology and geochemistry. *Reviews in Mineralogy*, 33, pp. 503–557.
- Henry D.J., Novák M., Hawthorne F.C., Ertl A., Dutrow B., Uher P. & Pezzotta F., 2011: Nomenclature of the tourmaline supergroup-minerals. *American Mineralogist*, 96, 895–913.
- Hoang L.H., Hien N.T.M., Chen X.B., Minh N.V. & Yang I.S., 2011: Raman spectroscopic study of various types of tourmalines. *Journal of Raman Spectroscopy*, 42, 1442–1446.
- Laurs B.M., Simmons W.B., Rossman G.R., Fritz E.A., Koivula J.I., Anckar B. & Falster A.U., 2007: Yellow Mn-rich tourmaline from the Canary mining area, Zambia. *Gems & Gemology*, 43, 4, 314–331.
- Laurs B.M., Zwaan J.C., Breeding C.M., Simmons W.B., Beaton D., Rijdsdijk K.F., Befi R. & Falster A.U., 2008: Copper-Bearing (Paraíba-Type) Tourmaline From Mozambique. *Gems & Gemology*, 44, 1, 4–30.
- Merkel P.B. & Breeding C.M., 2009: Spectral differentiation between copper and iron colorants in gem tourmalines. *Gems & Gemology*, 45, 2, 112–119.
- Nassau K., 1998: Color for Science, Art and Technology. Elsevier, Amsterdam, 491 p.
- Nasdala L., Smith D.C., Kaindl R. & Ziemann M.A., 2004: Raman spectroscopy: Analytical perspectives in mineralogical research. In: Beran A. & Libowitzky E. (Eds.): Spectroscopic methods in mineralogy, EMU Notes in Mineralogy, Eötvös University Press, pp. 281–343.
- Pieczka A., 2007: Blue dravite from the Szklary Pegmatite (Lower Silesia, Poland). *Mineralogia*, 38, 209–218.
- Reddy J., Frost R., Martens W., Wain D. & Klopogge T., 2007: Spectroscopic characterization of Mn-rich tourmalines. *Vibrational Spectroscopy*, 44, 42–49.
- Rossman, G.R., 2013: Mineral Spectroscopy Server. <http://minerals.gps.caltech.edu/index.html>
- Rossman G.R. & Mattson S.M., 1986: Yellow, Mn-rich elbaite with Mn-Ti intervalence charge transfer. *American Mineralogist*, 71, 599–602.
- Rossman G.R., Fritsch E. & Shigley J.E. (1991): Origin of color in cuprian elbaite from São José da Batalha, Paraíba, Brazil. *American Mineralogist*, 76, 1479–1484.
- RRUFF, 2014: RRUFF Project website. <http://rruff.info>
- Schmetzer K. & Bank H., 1979: East African tourmalines and their nomenclature. *Journal of Gemmology*, 16, 5, 310–311.
- Stockman A. & Sharpe L.T., 2000: Spectral sensitivities of the middle- and long-wavelength sensitive cones derived from measurements in observers of known genotype. *Vision Research*, 40, 1711–1737.